Determination of the Laminar, Structural and Disperse Shale Volumes Using a Joint Inversion of Conventional Logs*

Ambrosio Aquino-López[1], Aleksandr Mousatov[1], Mikhail Markov[1], and Elena Kazatchenko[1]

Search and Discovery Article #41944 (2016)**
Posted November 21, 2016

*Adapted from extended abstract based on poster presentation given at AAPG 2016 International Convention and Exhibition, Cancun, Mexico, September 6-9, 2016

[1]Gerencia de Geofísica Cuantitativa, Instituto Mexicano del Petróleo, Ciudad de México, Distrito Federal, México (aaquino@imp.mx)

Abstract

The determination of the volumes of disperse, structural and laminar shale is a challenging problem in the clastic-rock characterization. For this purpose, we have developed a technology to estimate spatial shale distribution to improve the assessment of hydrocarbon saturation and permeability prediction. This technology includes the simulation of physical properties of clastic rocks by introducing a unified hierarchical petrophysical model for shaly-sands and the joint petrophysical inversion of conventional well logs. We consider clastic formations as a sequence of laminar-shale and sand layers. Sand layers are treated as porous composite materials containing: solid grains of quartz, structural shale, and pores filled with a mixture of oil, water, and disperse shale. For calculating the effective physical properties of this composite, we apply the self-consistent effective media method. We simulate the effective physical properties of shaly-sand formations by applying three-step homogenization. Firstly, we calculate the effective properties of pores composed of water, oil, and disperse shale. Then, the properties of sand layers are determined by using the pore effective properties obtained in the first step. Finally, the formation effective physical properties can be calculated. The determination of physical properties in the second step requires information about shapes of grains and pores that were determined by inversion procedure taking into account a set of experimental data. We have shown that the acoustic and electrical logs depend significantly on the volumes and spatial distribution of shales. Layered formations are transverse isotropic media and the elastic moduli and electrical resistivity are represented by tensors. We have validated the proposed technology on synthetic models with different levels of a random noise and experimental data. Application of this technology allows us to add new shale characteristics to the conventional evaluation parameters such as volumes and porosities of laminar, structural, and disperse shales. These characteristics improve the assessment of hydrocarbon saturations and permeability of clastic formations.

Introduction

The correct formation evaluation represents a challenging problem for non-conventional shaly-sand reservoirs such as shale gas, shale oil or deep water formations. Erroneous results in the determination of the petrophysical properties in clastic rocks are related with conventional interpretation techniques that do not consider spatial distribution of shale: disperse, structural, and laminar. All “conventional” models currently applied in well-log interpretation were developed for specific methods such as sonic, electrical or neutron logs that are not compatible.

That presents a serious problem in the characterization of shaly-sand formations.

The first model to estimate porosity and water saturation in clean sandstones was proposed by Archie (1942). Later, different models for shaly sands that use solely the electrical resistivity have been developed (Poupon et al., 1954; Waxman and Smits, 1968; Clavier et al., 1984; Shevnin et al., 2007). Most of these authors focused on the influence of electrochemical phenomena of shales on the electrical conductivity of sandstones formations, but did not consider the spatial distribution of shale.

Based on the elastic wave properties, Wyllie et al. (1956) proposed a volumetric approach to determine the formation porosity. Raymer et al (1980) obtained a non-linear relation to improve the determination of porosity. Different authors (Castagna et al., 1985; Han, 1986; Marion, 1990) obtained regression equations between P- and S- wave velocities and total porosity taking into account the total volume of shale by applying statistical analysis on core data,.

Some authors applied micromechanical methods for petrophysical evaluation of clastic rocks (Sheng 1991, Han, et al., 2011) and of carbonate rocks (Kazatchenko et al., 2004) using different physical properties simultaneously. The models with different shale distribution in clastic rocks were considered by various authors to simulate only one physical property. Berg (2007) simulated the electrical resistivity by considering a model with disperse shale. Song and Tang (2008) analyzed the problem for the low resistivity reservoirs by using a generalized effective medium, considering disperse, structural and laminar shale, free water, hydrocarbon and bound water. Gelius and Wang (2008) used the differential effective medium method (DEM) to model shaly sands with hydrocarbon content. The effect of different shale distributions (disperse and structural) on elastic wave velocities was analyzed by Minear (1982).

In this paper, we propose a new technique for the joint inversion by using conventional well logs for the petrophysical evaluation of terrigenous formations. Our technique allows us to determine the shale volumes of different spatial distributions (disperse, structural and laminar) and water saturation. It is based on a hierarchical model that considers three homogenization levels: 1) pores that contain water, hydrocarbon and disperse shale, 2) sandstones formed by quartz, structural shale and pores (with the effective physical properties estimated in the first homogenization level) and 3) formation composed by layers of sandstones and laminar shale.

We apply the EMA method to calculate effective physical properties at the first two homogenizations levels. The procedure for determining the shapes is described in Aquino et al. (2011) for clean sandstones and in Aquino et al. (2015) for shaly sands. Layered formations (third homogenization level) are transverse isotropic media and the elastic moduli and the electrical resistivity are tensors. Our method allows simulation of the physical properties such as electrical resistivity, acoustic velocities, density, and gamma radioactivity.

We used the joint inversion of conventional well-log data to obtain the shale volumes of different spatial distributions and hydrocarbon saturations. The applied procedure was minimization of a cost function that consists of a weighted sum of the squares differences of experimental and predicted data. We applied our proposed technique to measured well data and obtained acceptable predictions of the physical properties measured in boreholes. We also compared the petrophysical evaluation after the inversion with results from the interpretation of non-conventional data, and obtained a good agreement as well.

Model and Simulation Method

We present shaly-sand formations by hierarchical model of three homogenization levels (Figure 1): 1) pore space (containing water, hydrocarbon and disperse shale), 2) sandstone layer (quartz and shale grains), and 3) formation (layers of laminar shales and sandstones). To calculate the effective electrical and acoustic properties of the pore-saturating fluid and sandstone on the first and second levels we use the micromechanical method of the effective media approximation (EMA). On the first homogenization level, the components of the saturating fluid (water, hydrocarbon) are taken as sphere. Based on theoretical calculations it was shown that the shape of disperse shale and structural shale weakly affected the elastic and electrical properties in range of interest of porosity in clastic rocks (Aquino et al., 2015). On the second homogenization level, we use the shape of pores and quartz grains obtained by Aquino, et al. (2011). On the third homogenization level, we consider a transversely isotropic medium composed by layers of shale and sand. The axis of macroscopic anisotropy is perpendicular to the stratification in this case.

Joint Inversion of Conventional Logs

The joint inversion uses conventional well logs: acoustic travel times (P- and S- wave velocities), electrical resistivity, bulk density, porosity, and gamma-ray radioactivity. We solve the optimization problem for the cost function (equation 1) at each point of the measurements k in a borehole:

$$F_k(S_{hc}, V_{dis}, V_{st}, V_{lam}, \phi_{sh}, \phi_{sd}) = w_{GR}(GR - GR^*)^2 + w_\rho(\rho - \rho^*)^2 + w_\phi(\phi_t - \phi_t^*)^2 + w_{Vp}(V_P - V_P^*)^2 + w_{VS}(V_S - V_S^*)^2 + w_R(\log R - \log R^*)^2 \quad (1)$$

where S_{hc} is hydrocarbon saturation; V_{dis}, V_{st} and V_{lam} are volumes of disperse, structural, and laminar shale, respectively; ϕ_{sh} and ϕ_{sd} are the porosities of shale and sand, respectively; GR is measured gamma ray; ρ is measured bulk density; ϕ is measured total porosity; V_p and V_s are P- and S-wave velocities, respectively; R is measured resistivity. Superscript index * corresponds to the synthetic logs. Parameters w_{GR}, w_p, w_ϕ, w_{Vp}, w_{Vs}, and w_R are the weight coefficients determined by the measurement accuracy and log quality. The coefficients are calculated as a function of the standard deviation for measured data. We adjust these coefficients during the inversion procedure using the analysis of the normalized-error distributions. We obtained the solution of the inversion problem using the standard algorithm of conjugate gradients (Gill et al., 1995).

Inversion for Synthetic Data

We verify the proposed inversion procedure with a theoretical model that represents layered clastic formations. Each layer is characterized by different volumes of laminar, structural, and disperse shale, hydrocarbon saturation, and porosity of shale and sand layers. Synthetic logs contain 3% of random noise. The inversion results show all parameters are estimated with a high confidence (Figure 2).

The accuracy of the joint inversion was evaluated by means of the adjusting errors: the difference between the model and predicted volumes normalized to its standard deviation (δ). The normalized errors for all parameters have a normal distribution with the mean equal to zero and its deviations are in the range of ±0.4, which confirms the correct estimation of the petrophysical parameters (Figure 3). Given these results, we consider that the presented petrophysical model adequately describes shaly-sand formations and the proposed technique of joint-inversion can be applied to experimental well-log data for formation characterization.

Inversion of experimental well logs: Case 1

The input information for well A includes Gamma Ray (GR), Horizontal Electrical Resistivity (Rh), P- and S-wave travel times (DTP and DTS, respectively), Bulk Density, and Neutron Porosity (Figure 4, tracks 1-6). Table 1 shows the physical parameters of the model components that we use in the inversion. Inversion results are shown in Figure 4: Track 7: Sand porosity and Shale porosity; 8: Laminar Shale, Structural Shale, Disperse Shale and Hydrocarbon Volumes; 9: Gas Saturation.

Simulated data (points in Figure 4; tracks 1-6) are very close to the measured logs (solid lines). The volumes of structural and disperse shale vary from 0 to 10% and laminar shale is close to zero except at depth XX480 m, where shale volume achieves 50% (Figure 4, track 8). Shale porosity slightly varies from 18 up to 23% and sand porosity is close to 20% in the interval XX440-XX460 m and then increases up to 35% at depth XX480 m. The porosity decreases at this depth by 17% followed by an increase to 27% at the bottom (Figure 4, track 6).

The majority of deviations are in the range ±0.5 of standard deviation. Correctness of the obtained microstructural model and saturating fluids is confirmed by comparison of gas saturation estimated by inversion with sidewall sampling data (Figure 4, track 9). The median values of the gas saturation are 5.1% and 4.4% respectively.

Inversion for experimental (real) data: Case 2

The input information for well B includes Gamma Ray, Horizontal and Vertical Electrical Resistivity, P- and S-wave travel times (DTP and DTS, respectively), Bulk Density, and Neutron Porosity (Figure 5, tracks 1-6). We did not include the vertical resistivity in the inversion process and used it to verify a formation model obtained by joint inversion. The physical parameters of the components used in the inversion are shown in Table 2.

Two washout zones are located in the processed interval (shaded areas in Figure 5). The effect of these zones on density, neutron porosity, and acoustic velocities leads to deterioration of the inversion and increases the adjustment errors. Nevertheless, taking into account the effect of the washout zones on the logs, we can consider a correct realization of the inversion procedure. The majority of errors are in the range of ±1 standard deviation. The resistivity log is adjusted well enough with errors in the interval -0.3 - 0.7 of standard deviation of the measured data. It should be noted that in the upper washout zone the resistivity increases in spite of the increment of volume of the conductive water. This is due to the variation of the rock microstructure – an abrupt decrease (up to zero) of the laminar-shale volume (Figure 5, track 7).

The shale distribution obtained after the joint inversion is presented in Figure 5, track 7. The volume of structural shale is below 10% with exception of two intervals at depth XX13 and XX23 m, where shale concentration increases up to 20%. Disperse shale is almost constant in all intervals (15-20%), and the presence of laminar shale is close to 25-35% with strong reduction at depth XX13. Shale and sand porosities are close and vary slightly from 18 to 25% (Figure 5, track 8). Determined shale distribution and water saturations are confirmed by data of the tri-axial induction log and nuclear magnetic resonance (Figure 6, tracks 4-5). One can observe a good coincidence of the inversion results with independently determined shale volumes and water saturation (Figure 6, track 7), obtained by using unconventional tools.

For well B we calculate the vertical resistivity based on the obtained formation model and compare it with the vertical resistivity log (Figure 6, track 6). The predicted and measured vertical resistivity coincides with a high degree of accuracy, which is an indicator of the adequate petrophysical model obtained by the joint inversion. The small difference between vertical and horizontal electrical resistivity denotes a low anisotropy, that, according to the inversion results, are explained by the presence of laminar shale (25-35%). The absence of anisotropy (R_H=R_V) at depth XX13 m is confirmed by the inversion results due to the absence of laminar shale. It is very important to note that inversion results are comparable with interpretation of advances logs (Figure 6, tracks 4, 5, and 7).

Conclusions

We have presented the technique of well-log joint inversion to determine the volumes of disperse, structural, and laminar shale, and to estimate the hydrocarbon saturation in shaly-sand rocks. The technique considers the hierarchical petrophysical model and joint inversion of conventional well logs. The inversion procedure includes a solution of the optimization problem for the following logs: electrical resistivity, acoustic velocities, gamma radioactivity, formation density, and porosity. We have successfully verified the proposed technique on the synthetic model with 3% of random noise and applied it to the experimental well-log data. In addition to the determination of petrophysical parameters and formation microstructure, the technique allows predicting missing logs, e.g. we can reconstruct the vertical resistivity log from the available conventional data. The technique developed significantly improves the evaluation of shaly-sand formations providing additional parameters such as shale and sand porosities. The separation of shales by the spatial distribution allows petrophysicists to obtain the correct evaluation of oil and gas saturations, hydraulic permeability (through the effective porosity), and localization of impermeable zone (laminated shale).

References Cited

Aquino-López, A., A. Mousatov, and M. Markov, 2011, Model of sand formations for joint simulation of elastic moduli and electrical conductivity: J. Geophys. Eng., v. 8, p. 568-578.

Aquino-López, A., A. Mousatov, and M. Markov, 2015, Modeling and inversion of elastic wave velocities and electrical conductivity in clastic formations with structural and disperse shales: Journal of Applied Geophysics. http://dx.doi.org/10.1016/j.jappgeo.2015.02.013.

Archie, G.E., 1942, The electrical resistivity log as an aid in determining somo reservoir characteristics: Trans. AIME, v. 146, p. 54-62.

Berg, C., 2007, An effective medium algorithm for calculating water saturations at any salinity or frequency: Geophysics, v. 72/2.

Castagna, J.P., M.L. Batzle, and R.L. Eastwood, 1985, Relationships between compressional-wave and shear-wave velocities in clastic silicate rocks: Geophysics, v. 50, p. 571–581.

Clavier, C., G. Coates, and J. Dumanoir, 1984, Theoretical and experimental bases for the dual-water model for interpretation of shaly sands: SPE Journal, v. 24, p. 153-168.

Gelius, L.J., and Z. Wang, 2008, Modelling production caused changes in conductivity for a siliciclastic reservoirs: a differential effective medium approach: Geophysical Prospecting, v. 56, p. 677-691.

Gill, P.E., W. Murray, and M.H. Wright, 1995, Practical optimization: Academic Press, London, San Diego, 401 p.

Han, D.H., 1986, Effects of porosity and clay content on acoustic properties of sandstones and unconsolidated sediments: PhD thesis, Stanford University.

Han, T., A.I. Best, L.M. MacGregor, J. Sothcott, and T.A. Minshull, 2011, Joint elastic-electrical effective medium models of reservoir sandstones: Geophysical Prospecting, v. 59, p. 777-786.

Kazatchenko, E., M. Markov, and A. Mousatov, 2004, Joint inversion of acoustic and resistivity data for carbonate microstructure evaluation: Petrophysics, v. 45/2, p. 130-140.

Marion, D.P., 1990, Acoustical, mechanical and transport properties of sediments and granular materials: PhD thesis, Stanford University.

Minear, J.W., 1982, Clay models and acoustic velocities: Presented at the 57th Ann. Mtg., Am. Min. Metall. Eng., New Orleans.

Poupon, A., M.E. Loy and M.P. Tixier, 1954, A contribution to electrical log interpretation in shaly sands: Journal of Petroleum Technology, T.P. 3800.

Raymer, L.L., E.R. Hunt, and J.S. Gardner, 1980, An improved sonic transit time-to-porosity transform: SPWLA 21th Annual Logging Symposium, Paper P.

Sheng, P., 1991, Consistent modeling of the electrical and elastic properties of sedimentary rocks: Geophysics, v. 56, p. 1236-1243.

Shevnin V., A. Mousatov, A. Ryjov, and O. Delgado-Rodriguez, 2007, Estimation of clay content in soil based on resistivity modelling and laboratory measurements: Geophysical Prospecting, v. 55, p. 265-275.

Song, Y.J., and X.M. Tang, 2008, Generalized effective medium resistivity model for low resistivity reservoir: Science in China Series D: Earth Sciences, v. 51, p. 1194-1208.

Waxman, M.H. and L.J.M. Smits, 1968, Electrical conduction in oil-bearing sands: Society of Petroleum Engineers Journal, v. 8, p. 107-122.

Wyllie, M.R.J., A.R. Gregory, and I.W. Gardner, 1956, Elastic wave velocities in heterogeneous and porous media: Geophysics, v. 21/1, p. 41-70.

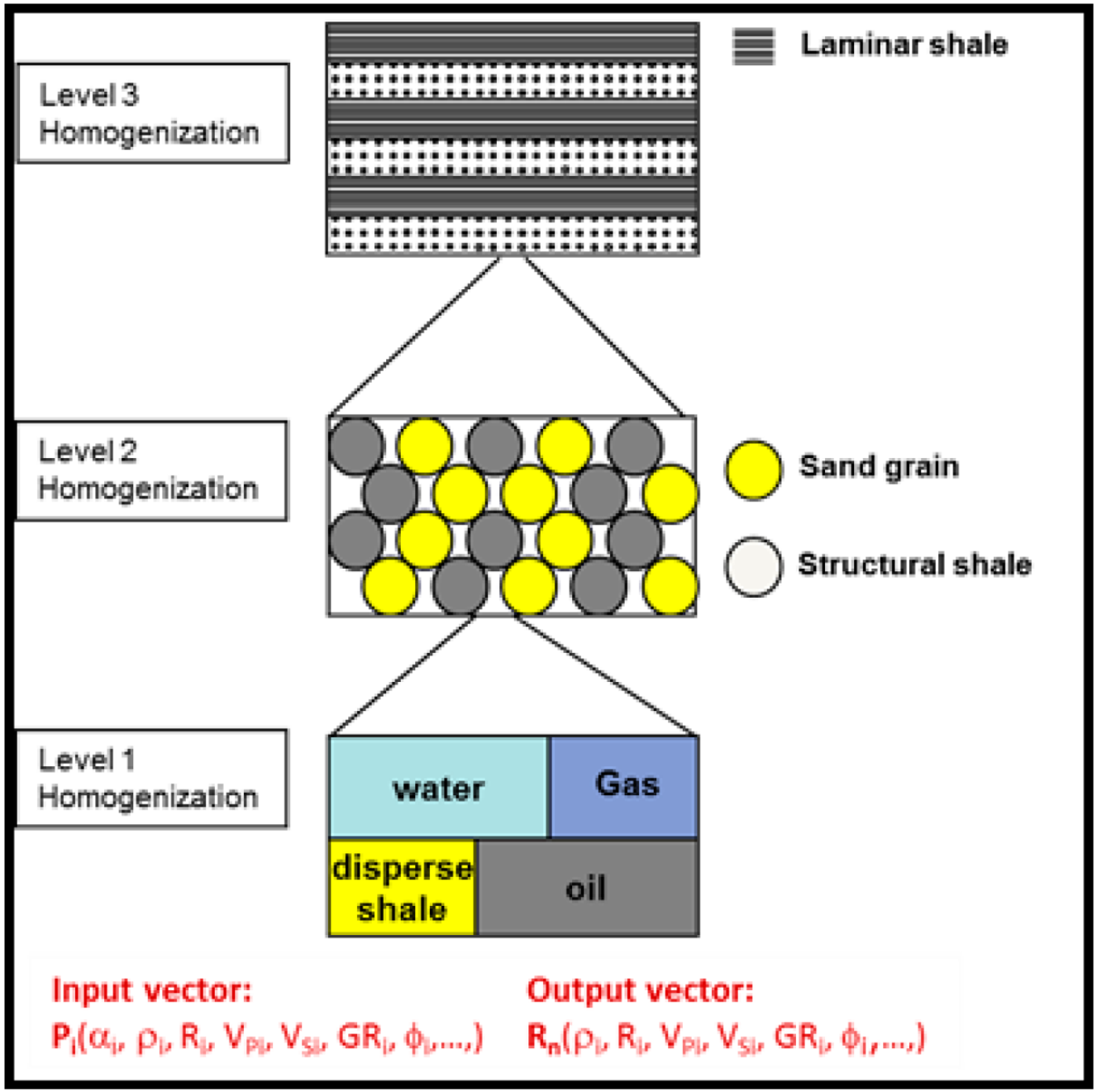

Figure 1. Hierarchical petrophysical model for clastic rocks.

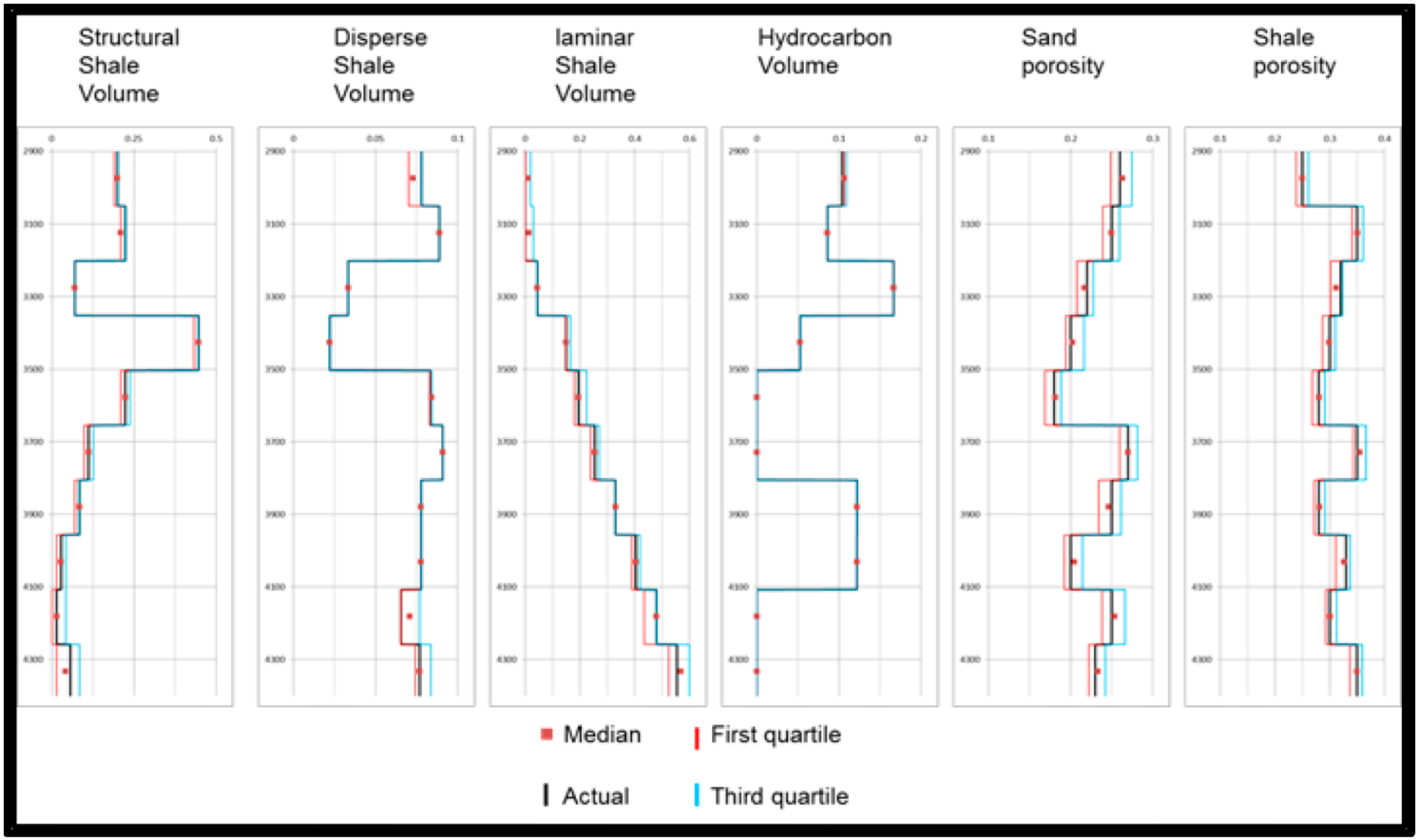

Figure 2. Inversion results for the synthetic model with 3% of random noise.

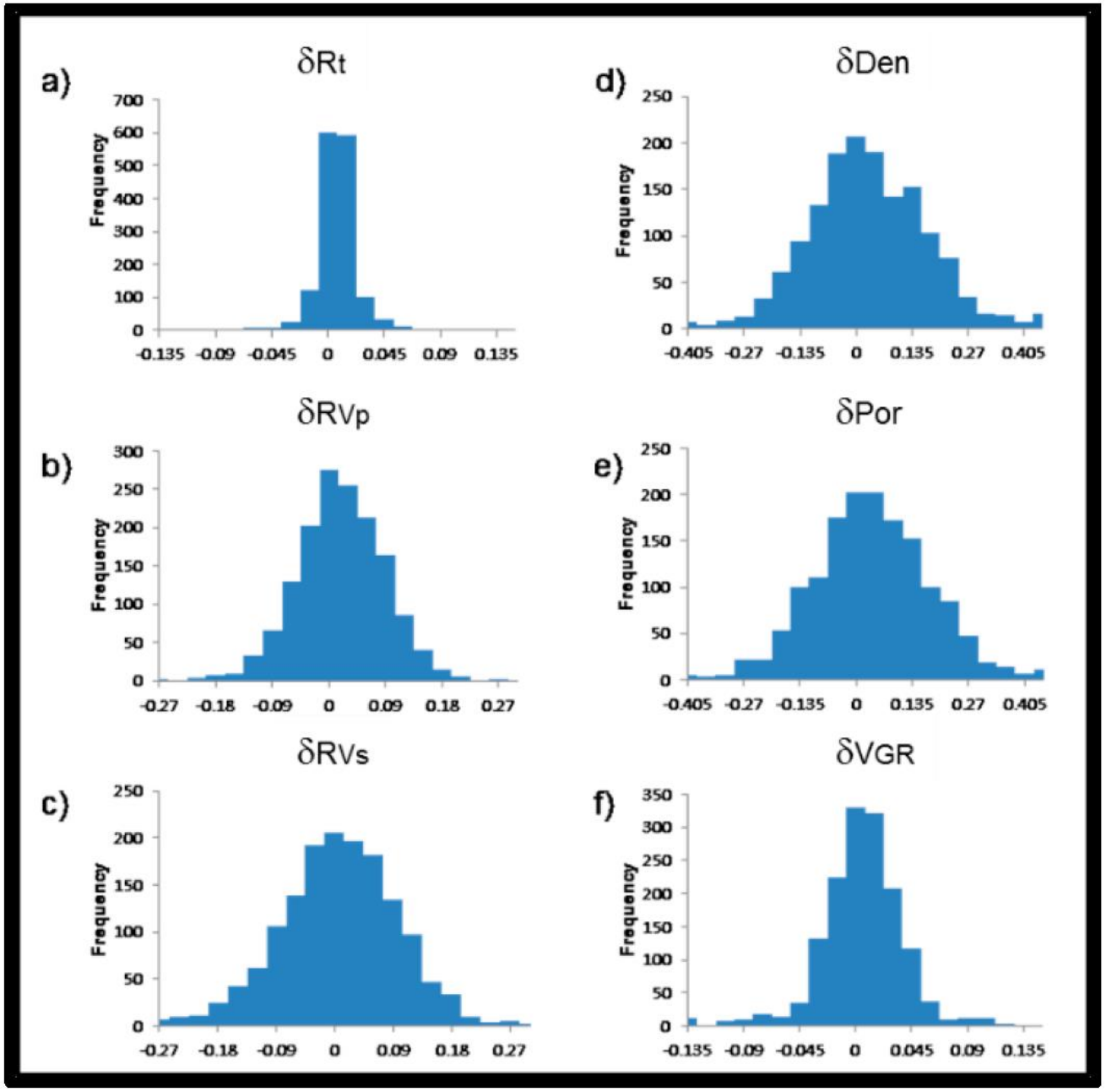

Figure 3. Histograms of the normalized errors of the predictions: (a) electrical resistivity (δ_{Rt}), (b) P (δ_{Vp}) - and (c) S (δ_{Vs})-wave velocities, (d) density (δ_{Den}), (e) total porosity (δ_{Por}) and (f) gamma ray (δ_{GR}) for the synthetic model with 3% of noise.

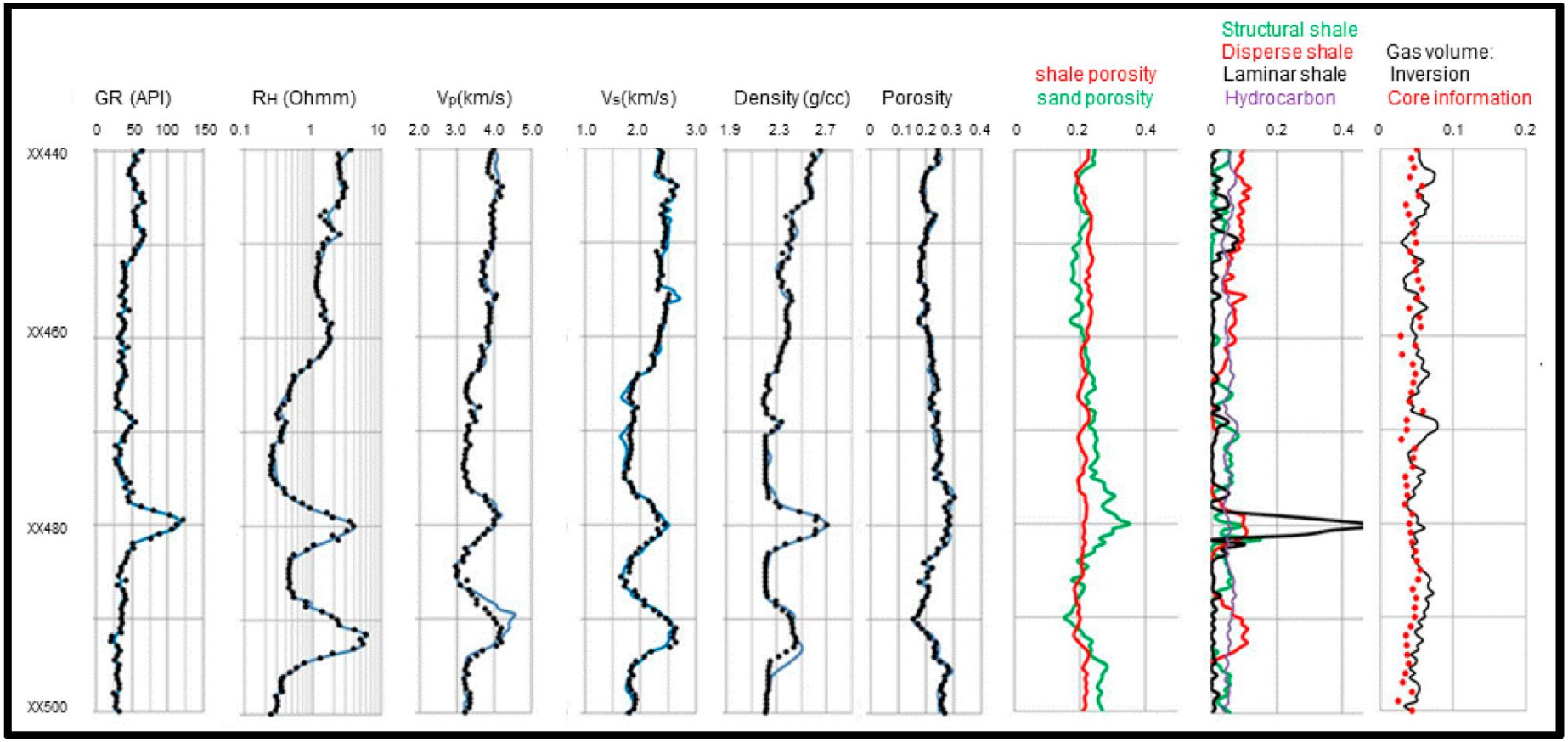

Figure 4. Measured and simulated data for Well A. Track 1: Gamma ray; 2: Horizontal electrical resistivity; 3: P-wave velocity; 4: S-wave velocity; 5: Bulk Density; 6: Neutron porosity. Inversion results are shown: Track 7: Sand porosity and shale porosity; 8: laminar shale, structural shale, disperse shale and hydrocarbon volumes; 9: gas volume.

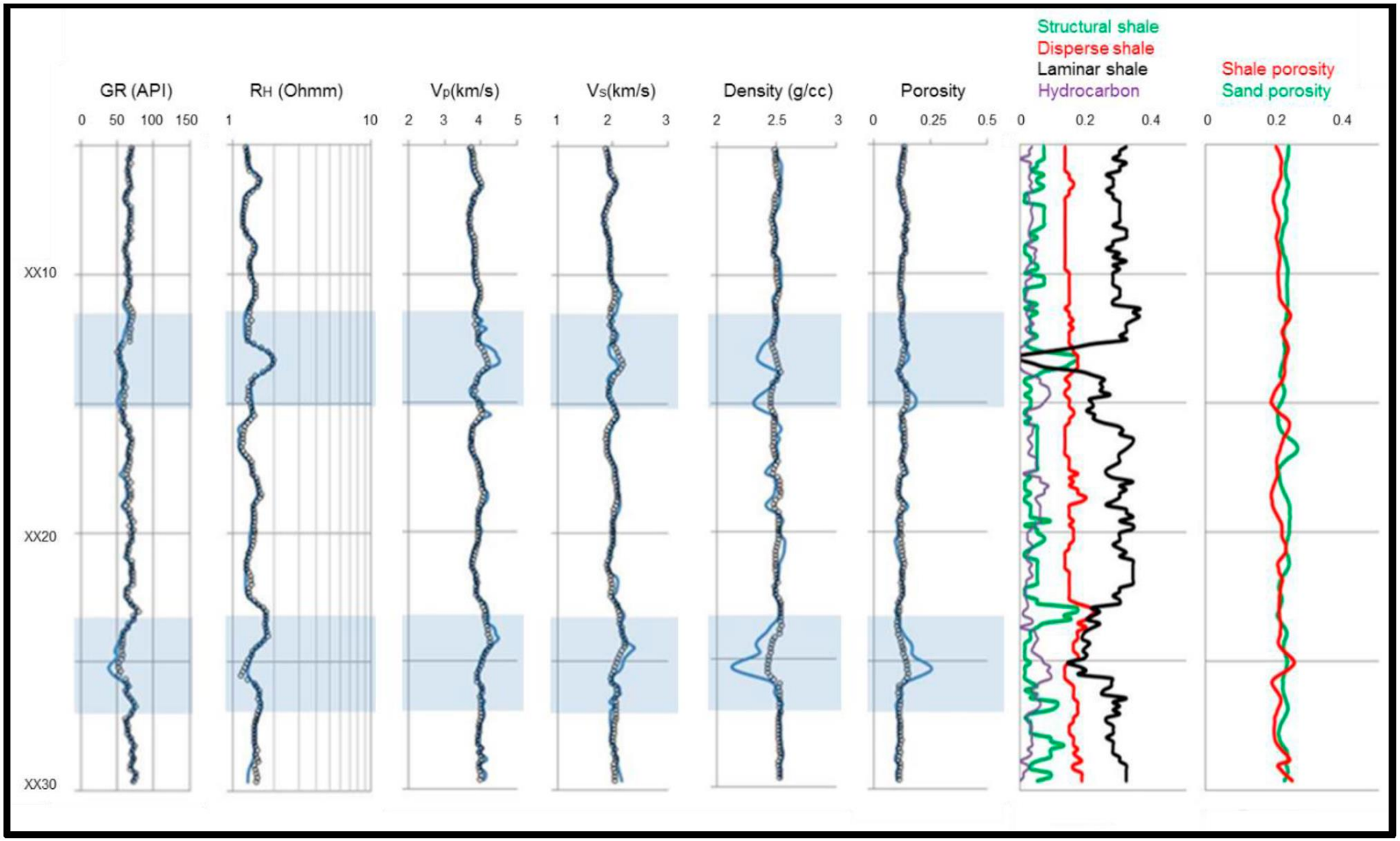

Figure 5. Measured and simulated data for Well A. Track 1: Gamma ray; 2: Horizontal electrical resistivity; 3: P-wave velocity; 4: S-wave velocity; 5: Bulk density and 6: Neutron porosity. Inversion results are shown: Track 7: laminar shale, structural shale, disperse shale and hydrocarbon volumes; 8: Sand porosity and shale porosity.

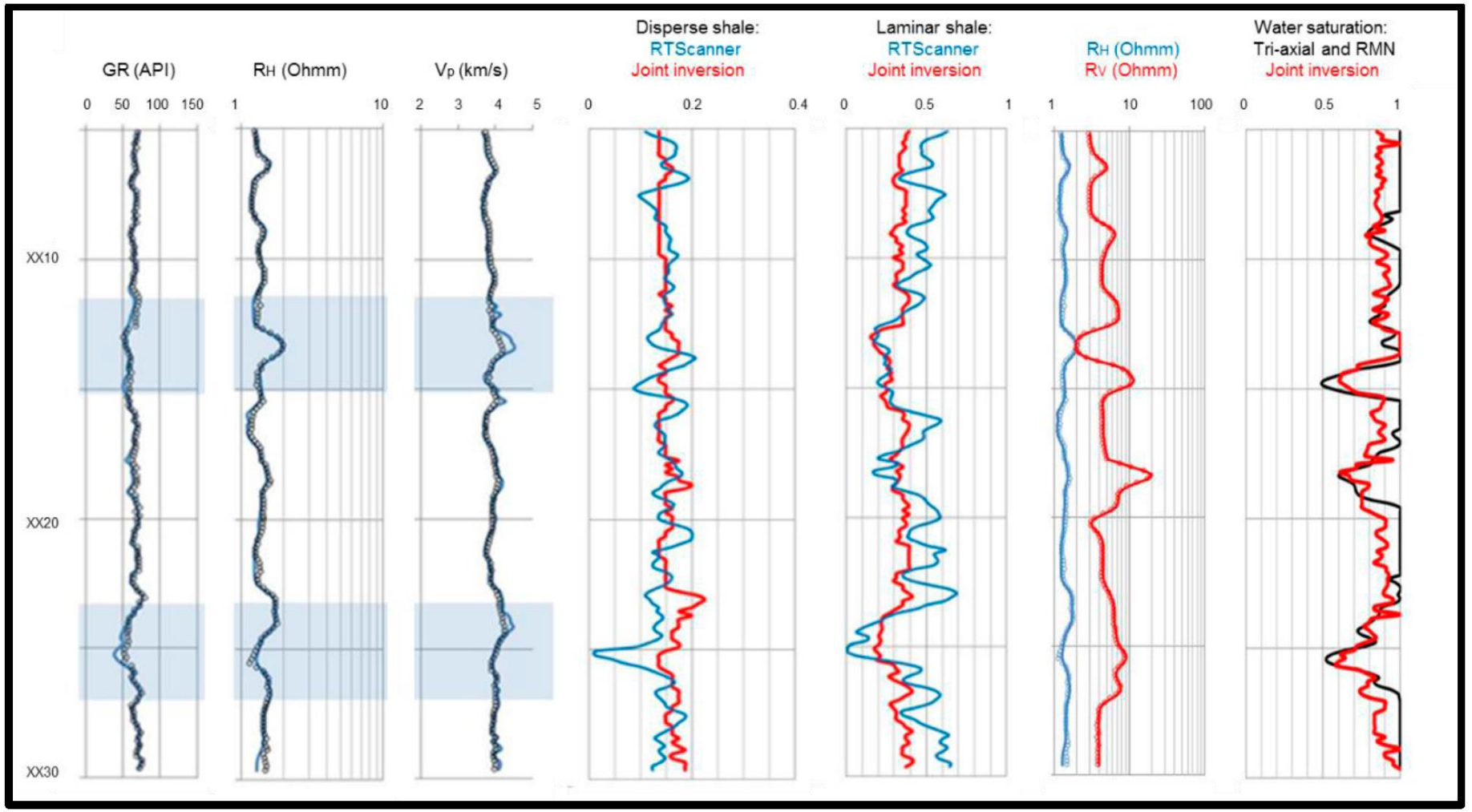

Figure 6. Measured and simulated data for Well A. Track 1: Gamma ray; 2: Horizontal electrical resistivity; 3: P-wave velocity; 4: disperse shale obtained by inversion and NMR; 5: laminar shale obtained by inversion and NMR; 6: horizontal and vertical resistivities (measured and simulated) and 7: Water saturation by inversion and with NMR and triaxial-tool.

Component	DTP (μs/ft)	DTS (μs/ft)	Density (g/cm^3)	Electrical resistivity (Ohm.m)
Gas	900	166666	0.08	$1x10^9$
Water	200	166666	1.0	0.1
Shale	110	188	2.4	1.0
quartz	55	88	2.64	$1x10^{14}$

Table 1. Parameters of the model involved in the inversion process.

Component	DTP (μs/ft)	DTS (μs/ft)	Density (g/cm^3)	Electrical resistivity (Omm)
oil	215	166666	0.8	$1x10^9$
water	200	166666	1.0	0.1
shale	110	188	2.4	1.0
quartz	55	88	2.64	$1x10^{14}$

Table 2. Parameters of the model involved in the inversion process.